Synthesis, characterization and application of undoped TiO$_2$ and co-doped TiO$_2$ (with Ba & Co) for the photocatalytic degradation of Coomassive brilliant blue (CBB) dye under UV light irradiation

F. Akbar Jan[1]*, Sh. Khalid[1], N. Ullah[2], R. Ullah[1]

[1]*Department of Chemistry, Bacha Khan University Chrasadda, Khyber-Pakhtunkhwa, 24420 Pakistan*
[2]*Department of Chemistry, Qauid-i-Azam University Islamabad, 45320 Pakistan*

Titanium oxide (TiO$_2$) and Ba and Co co-doped TiO$_2$ nanoparticles were synthesized through a sol-gel method. The synthesized nanoparticles were characterized using X-ray diffraction (XRD), Fourier transform infrared spectroscopy (FTIR), UV-visible spectroscopy (UV-Vis), and scanning electron microscopy (SEM). Using X-ray diffraction analysis different parameters were calculated, such as crystallite size, d-spacing, dislocation density, number of unit cells, cell volume, morphological index, microstrain and instrumental broadening. The average particle size of both titanium oxide (TiO$_2$) and Ba and Co co-doped TiO$_2$ nanoparticles was calculated to be 15.98 nm and 24.69 nm, respectively. Scanning electron microscopy revealed that TiO$_2$ has rough spherical morphology with small particles agglomeration while Ba and Co co-doped TiO$_2$ nanoparticles consist of slightly larger blocks of agglomerated particles with irregular morphology. Doping of TiO$_2$ with Ba and Co decreased the band gap from 3.10 eV to 2.92 eV. The characterized particles were used as a photocatalyst for the degradation of Coomassive brilliant blue dye in aqueous solution under UV light. The effect of different parameters, e. g. irradiation time, initial dye concentration, pH of the medium and catalyst dosage on the percent degradation was also studied. The dye degradation linearly increased with an increase in irradiation time. About 93% and 77% dye degradation was observed at 240 min duration using undoped and Co-Ba-doped TiO$_2$, respectively. The degradation of the dye was found to decrease with an increase in initial dye concentration. On increasing the amount of Co-Ba-doped TiO$_2$ catalyst the rate of degradation increased while using bare TiO$_2$ the percent degradation decreased with increase in catalyst dose up to 0.05 g. At low pH higher degradation was found as compared to higher pH. Co and Ba co-doped TiO$_2$ powders exhibited high photocatalytic activity towards discoloration of Coomassive brilliant blue dye.

Keywords: Titanium oxide (TiO$_2$), Ba and Co co-doped TiO$_2$, nanoparticles, Coomassive brilliant blue dye, UV light

INTRODUCTION

Modern textile and dyeing industries have led to the direct or indirect dumping of more and more toxic substances to air and water thereby threatening environment and humanity [1]. There is a dire need for the removal of dyes from local and industrial water effluents with cost-effective technologies in compliance with growing environmental rules and regulations. Coomassive brilliant blue dye belongs to the group of non-azo dyes and is used as an acid wool dye. It is also used as a reagent for staining proteins in electrophoresis techniques and for measuring protein [2]. Coagulation by chemical agents and resins, activated carbon, electro catalytic decomposition, ultrafiltration and biological treatment are wastewater treatment technologies currently in use [3]. The dyes are resistant to biological, as well as physical treatment technologies[4]. The other methods have their own demerits but advanced oxidation processes (AOP) which are used for the photodegradation of toxic compounds have gained the attention of scientists in recent years [5]. Semiconductor material-based photocatalysts have been extensively used in the fields of solar energy conversion, cleaning and sterilization, sewage treatment and air purification. Production of no secondary pollutants, mild reaction conditions, high efficiency and high stability and complete mineralization of pollutants are among the merits of the photocatalytic oxidation process over the other techniques. Constructing an efficient photocatalyst with visible light response and conducting an in-depth study of its mechanism is required now-a-days to boost the efficiency of the waste water purification process [6]. Both homogenous and heterogeneous catalysis are used for the degradation of various families of hazardous materials [7]. Photocatalytic degradation using a nanocatalyst has been employed as a preferred effective method for the demineralization of organic pollutants. Nanomaterials have unique properties, i.e., large surface area, ease of preparation and wide energy gaps which can be altered by doping with other metals. A number of compounds including

---

* To whom all correspondence should be sent:
E-mail: fazal_akbarchem@yahoo.com

ZnO, SnO$_2$ and ZnO$_3$ are used for photocatalytic degradation. Titanium dioxide is one of the important candidates for nanomaterials. It is relatively safe, nontoxic, and cheap, it is also used as a whitening ingredient in toothpastes. It is used in photochemistry ranging from large-scale products to more advanced applications including dye-sensitized solar cells, photoelectrolysis of water and environmental remediation[8, 9]. Owing to its large band gap (3–3.2eV) the efficiency of TiO$_2$ is limited to the UV range [10]. In order to improve degradation and recovery efficiency, both metal and non-metal oxides are doped and co-doped with it. Doping causes shifting of both the conduction band (CB) and valence band (VB) of TiO$_2$ to more negative values resulting in the formation of $\cdot O^{2-}$ which significantly enhances photodegradation. Photodegradation efficiency is also affected by carrier separation, and transfer reduction potential [11]. As the conduction band of TiO$_2$ is higher in energy than the Fermi level of the noble metal, thus photo promoted electrons can efficiently migrate to the metal, leaving holes in the TiO$_2$ valence band [12]. Studies have reported the degradation of toluene and methylene blue under visible light using Zr, S and B, Zr co-doped TiO$_2$ [13]. Co-doping of TiO$_2$ using Ba, Zr and Co has drawn the attention because these dopants not only increase the surface area but also thermally stabilize the TiO$_2$ which retards the combination of electrons and holes. Less dense anatase phase TiO$_2$ formation is facilitated by Ba^{2+} due to its more electropositive nature and hence high photocatalytic activity. The effect of elements with large ionic radii: Ba^{2+}(1.3 Å), Zr^{3+} (0.79 Å) and Zr^{4+} (0.68 Å) has also been studied while using them for the photocatalytic degradation of the pollutant dye Rhodamine B [14]. Keeping in view the advantages of co-doping a study was designed to synthesize and characterize undoped TiO$_2$ and Ba &Co co-doped TiO$_2$. Application of bareTiO$_2$ and co-doped TiO$_2$ NPs for the photocatalytic degradation of Coomassive brilliant blue dye in aqueous medium was among the objectives of the study.

EXPERIMENTAL

Synthesis of TiO₂ and doped TiO₂ nanoparticles (NPs)

TiO$_2$ nanoparticles were synthesized through sol gel technique. Figure 1 represents the schematic diagram for the synthesis of TiO$_2$ nanoparticles. First 4.21 ml of titanium (IV) iso-propoxide was added to 12 ml of iso-propanol and the mixture was stirred for 5 min using a magnetic stirrer. Thus, we got an alkoxide solution. A mixture of one ml water and five ml iso-propanol was prepared and added drop wise to the alkoxide solution. The mixture was then stirred for 24 h at ambient temperature. Upon completion of the reaction the precipitate was dried at 100 $^\circ$C in an oven. It was finally calcined at 500 $^\circ$C and 1000 $^\circ$C in a furnace. The above-mentioned sol-gel technique was also applied for the synthesis of Ba and Co co-doped TiO$_2$NPs with addition of 3% (1.5% of each dopant) of barium chloride and cobalt chloride hexahydrate salts to the TTIP solution before the hydrolysis step.

Characterization techniques

The synthesized nanoparticles were characterized using X-ray diffraction (XRD), scanning electron microscopy (SEM), energy dispersive X-ray (EDX), UV-Vis spectrophotometry and FTIR spectroscopy.
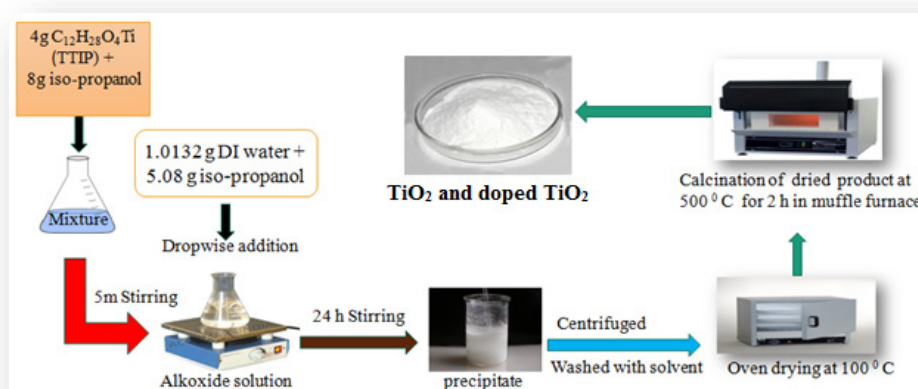
Fig. 1. Schematic diagram of the sol-gel method for the synthesis of TiO$_2$ and doped TiO$_2$NPs.

Preparation of the dye solution

The stock solution (500 ppm) of Coomassive brilliant blue dye (CBB) was prepared by dissolving 0.125 g of dry powder of dye in distilled water and vigorously shaking. Then working solutions of different concentrations were prepared from the stock solution. The working solutions were prepared using the dilution formula given in equation (1):

$$M_1V_1 = M_2V_2 \tag{1}$$

Photocatalytic degradation of dye

The photocatalytic activity of TiO₂ NPs and barium and cobalt co-doped TiO₂ NPs was evaluated in the degradation of the organic dye Coomassive brilliant blue in aqueous solution. For comparison the photocatalytic degradation of the dye was carried out under UV light and sun light. The maximum absorption of Coomassive brilliant blue dye was found at 556 nm and was used as a monitor wavelength for photodegradation. An appropriate amount (0.01 to 0.05 g) of photocatalyst was separately added to the working solutions. The mixed solution was stirred for 30 min in the dark to establish desorption/desorption equilibrium before the photodegradation reaction. Then the dispersion was kept in a light source. In the experiments an UV-lamp was placed 15 cm above the surface of the solution in a locally designed equipment. The dye degradation was checked at various intervals of time, and the catalyst was removed by centrifugation. The same process was repeated in sun light. The absorbance of the centrifuged solution was measured by UV-Vis spectrometry. The percent photodegradation of Coomassive brilliant blue dye was calculated using the following relation given in equation (2):

$$D(\%) = \frac{C_0 - C_t}{C_0} \times 100 \tag{2}$$

where C_0 and C_t denote the concentrations of Coomassive brilliant blue dye at time 0 min and t(s), respectively, and t is the irradiation time.

RESULTS AND DISCUSSION

XRD study

Figure 2 shows the XRD spectrum of the synthesized materials.

$$D = \frac{K\lambda}{\beta \cos \Theta} \tag{3}$$

where D is the crystallite size, K is the Scherrer constant having a value of 0.9, λ is the diffraction wavelength of light, β shows the full width at half maximum of sharp peaks and Θ is the angle of reflection.

The average crystallite sizes of undoped and doped TiO₂ are 15.98 nm and 24.69 nm, respectively.
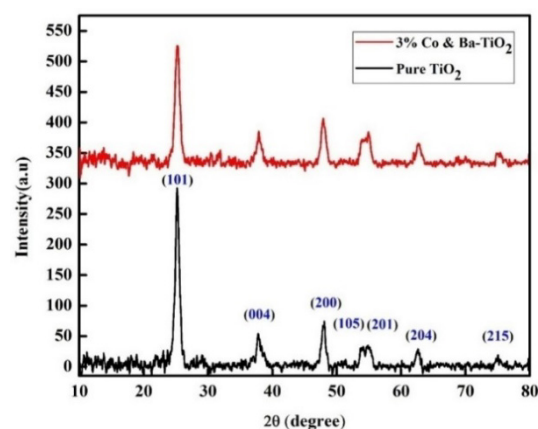
Fig. 2. XRD pattern of (a) TiO₂ and (b) Ba and Co co-doped TiO₂ nanoparticles.

XRD d-spacing

d-Spacing was calculated using Bragg's law; the d-spacing is the interplanar spacing between the two atoms shown in equation (4):

$$2\,d \sin \Theta = n\lambda \tag{4}$$

where λ is the wavelength of X-rays; its value is 1.5406 Å for CuKα [15]. The values of d-spacing for 2Θ positions at 25.16°, 37.84°, 48.09°, 53.91°, 55.06°, 62.70° and 75.07° for TiO₂ and for doped TiO₂ are 25.30°, 38.00°, 48.10°, 55.03°, 62.6°3 and 75.21° as shown in Tables 1 and 2.

XRD dislocation density

Dislocation is the irregularity or crystallographic imperfection within the crystal structure or a deviation from a perfect crystal structure. Material science well explains the numerous properties influenced by the presence of dislocation within the crystal. The movement of one dislocation hinders the other dislocations present in the crystal structure. Also, the bigger the dislocation the larger will be the hardness of sample [16]. The formula for calculation of dislocation density is shown in equation (5):

$$\delta = \frac{1}{D^2} \tag{5}$$

where δ represents the dislocation density and D is the crystallite size of the nanoparticles. The values of the dislocation density for TiO₂ and doped TiO₂ are shown in Tables 1 and 2.

Table 1. Diffraction angle, FWHM (β), particle size (D), d-spacing, dislocation density, number of unit cells and morphology index of TiO₂ nanoparticles.

Diffraction Angle (2θ in degree)	FWHMβ) (Radians)	Particle Size (D) (nm)	d-Spacing (Å)	Dislocation Density $(m^{-2}) \times 10^{-3}$	Number of Unit Cells $\times 10^{-3}$	Morphological Index (Unitless)
25.30	0.0068	20.44	2.80	2.40	33.91	0.59
38.00	0.0061	47.93	2.43	0.43	437.20	0.61
48.10	0.0050	31.59	1.91	1.00	125.18	0.64
55.03	0.0061	31.59	1.60	1.01	125.18	0.61
62.63	0.0064	21.71	1.45	2.23	40.63	0.60
75.21	0.0099	14.04	1.20	5.02	10.98	0.50

Table 2. Diffraction angle, FWHM (β), particle size (D), d-spacing, dislocation density, number of unit cells and morphology index of co-doped TiO₂ nanoparticles.

Diffraction Angle (2θ in degree)	FWHM(β) (Radians)	Particle Size (D) (nm)	d-Spacing (Å)	Dislocation Density $(m^{-2}) \times 10^{-3}$	Number of Unit Cells $\times 10^{-3}$	Morphological Index (Unitless)
25.16	0.0121	11.84	3.53	7.10	6.53	0.62
37.84	0.0054	27.80	2.37	1.23	85.31	0.78
48.09	0.0082	18.78	1.89	2.83	26.30	0.70
53.91	0.0082	19.30	1.70	2.60	27.27	0.70
55.06	0.010	14.32	1.66	4.81	11.66	0.64
62.70	0.016	10.69	1.48	8.72	4.63	0.55
75.07	0.020	8.68	1.26	13.20	2.50	0.50

The number of unit cells of the crystal system was calculated using the formula given in equation (6):

$$n = \pi \left(\frac{4}{3}\right)^x \left(\frac{D}{2}\right)^{3x} (1/V) \qquad (6)$$

There is an inverse relation of the number of unit cells with the dislocation density as shown by the equation($n = \frac{(constant)}{\delta^{\frac{3}{2}}}$). Dislocation density is a defect in which the layers of the crystals in the crystal lattice are dislocated from their original position. The graphical plot and the equation show that by increase in the number of unit cells the dislocation density of the lattice structure decreases.

The particle size is in direct relation with the number of unit cells. This is also confirmed by the relation between the particle size and the number of unit cells, $n = \pi(\frac{4}{3}) \times \left(\frac{D}{2}\right)^3 \times \left(\frac{1}{V}\right)$. Here the number of unit cells is in direct relation with the third power of the particle size.

XRD cell volume

TiO₂ has tetragonal crystal symmetry [17]. Known the values of space groups the cell volume of tetragonal crystal symmetry of TiO₂, doped TiO₂ can be calculated using equation (7):

$$V = a^2c \qquad (7)$$

where V is cell volume, and c represents the unit cell axis dimensions. The cell volume of TiO₂ and doped TiO₂ tetragonal system is $130.36 \times 10^6 m^{-3}$.

XRD morphological index

The morphological index for TiO₂ tetragonal system was calculated from FWHM of the XRD data. The formula for calculation of morphological index is given in equation (8):

$$M.I. = \frac{FWHM_h}{FWHM_h + FWHM_p} \qquad (8)$$

where M.I. represents the morphological index, $FWHM_h$ shows the highest FWHM value which was obtained from the peak. The values calculated for TiO₂ and doped TiO₂ tetragonal system are given in Tables 3 and 4.

XRD microstrain

Microstrain is defined as the variation across the individual crystallite lattice parameter in terms of root mean square. The microstrains of TiO$_2$ and doped TiO$_2$ tetragonal system were calculated using the formula shown in equation (9):

$$\varepsilon = \frac{\beta}{4\tan\Theta} \tag{9}$$

where ε is the microstrain and β represents the FWHM of the diffraction peaks. Moreover, the relationship between the microstrain and the broadening is due to micro deformation [18]. The value of the microstrain cannot be negative. The values for TiO$_2$ and doped TiO$_2$ tetragonal system are given in Tables 3 and 4. The FWHM of the strain parameter also increases.

Table 3. FWHM (β), and microstrain (ε) of TiO$_2$ nanoparticles.

FWHM(β) (Radians)	Microstrain (Unitless)
0.0068	0.052
0.0061	0.008
0.0050	0.002
0.0061	0.072
0.0064	0.014
0.0099	0.024

Table 4. FWHM (β), and microstrain (ε) of doped TiO$_2$ nanoparticles.

FWHM(β) (Radians)	Microstrain (Unitless)
0.0121	0.212
0.0054	0.019
0.0082	0.039
0.0082	0.005
0.010	0.062
0.016	0.061
0.020	0.25

XRD instrumental broadening

When the particle size is less than 100 nm then substantial broadening in X-ray diffraction line will happen. Broadening will occur in the diffraction pattern due to the reduction of crystallite size and strain in the crystal system [19]. Both instrument and sample broadening combined to form total broadening shown by equation (10):

$$\beta^2{}_D = [\beta^2{}_{measures} - \beta^2{}_{Instrumental}] \tag{10}$$

$$D = \frac{K\lambda}{\beta_D\cos\Theta} \text{ or } \cos\Theta = \frac{K\lambda}{D}\left(\frac{1}{\beta_D}\right) \tag{11}$$

$$\beta_{hkl} = \beta_s + \beta_D \tag{12}$$

where β_s is the sample broadening and β_D is the instrumental broadening.

$$\beta_{hkl} = \left(\frac{K\lambda}{\beta_D\cos\Theta}\right) + 4\,\varepsilon\tan\Theta \tag{13}$$

$$\cos\Theta\,\beta_{hkl} = \left[\left(\frac{k\lambda}{\beta_D}\right) + 4\,\varepsilon\sin\Theta\right] \tag{14}$$

Equation (14) stands for UDM (uniform deformation model) and means that the strain is uniform in all crystallographic directions, ε is the microstrain of the crystal system and instrumental broadening.

UV-Vis studies

Figure 3 shows the UV-Vis spectrum of the undoped TiO$_2$ and co-doped TiO$_2$ nanoparticles. The wavelength range of the spectrometer was set from 200 nm to 800 nm. The UV-Vis spectrum corresponding to undoped TiO$_2$ NPs dispersed in deionized water shows a broad absorption peak at 297 nm with a fundamental edge of absorption at 512 nm, which is formed by extrapolating the straight line to come across the X-axis. In the UV-Vis spectrum of the co-doped NPs a maximum absorption band appeared at 220 nm with a fundamental edge of absorption shifted toward higher wavelengths. The results show a red shift in the spectrum as compared to undoped TiO$_2$ NPs.
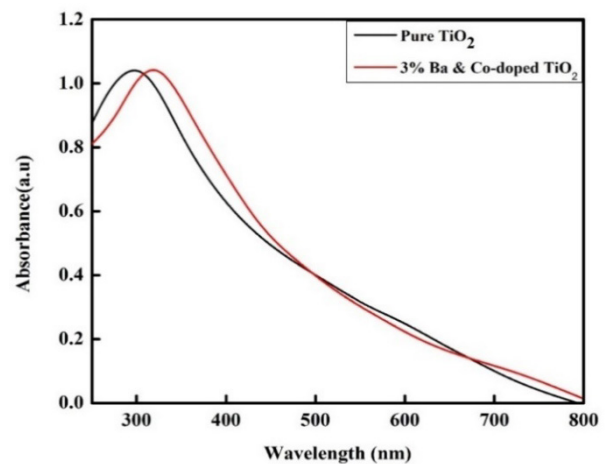
Fig. 3. UV-Vis spectra of TiO$_2$ and Ba-Co co-doped TiO$_2$ nanoparticles.
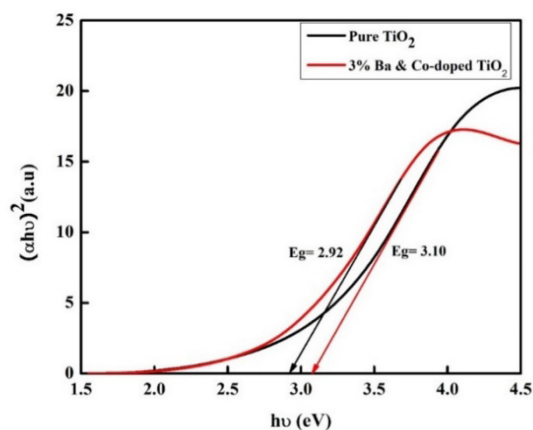
Fig. 4. Band gaps of TiO$_2$ and Ba-Co co-doped TiO$_2$ nanoparticles.

Band gap

The band gap values of undoped TiO$_2$ NPs and co-doped TiO$_2$ NPs were calculated using UV-Vis spectroscopic data as shown in Figure 4. The concerned equation (15) is given below.

$$\alpha h\upsilon = A(h\upsilon - Eg)^n \qquad (15)$$

where α is the absorption coefficient, υ is the energy of photon, A is the proportionality constant, n is the transition index. The band gap values of TiO$_2$ and doped TiO$_2$ NPs came out to be 3.10 eV and 2.92 eV, respectively. The results show tuning in the band of doped TiO$_2$ as compared to undoped TiO$_2$ NPs.

FTIR studies

FTIR measurements were performed over the wave number range of 400-4000 cm^{-1}. Figure 5 shows the FTIR spectrum of undoped and doped TiO$_2$ NPs calcined at 500 °C. Small peaks in the range of 400-1000 cm^{-1} reveal the formation of anatase phase of TiO$_2$ NPs corresponding to bending mode of Ti-O-Ti. The broad peak at 3461 cm^{-1} corresponds to the O-H stretching of the alcohol solvent. The symmetric stretching vibration of the carboxylate group occurs at 1435 cm^{-1}. The symmetric and asymmetric vibration modes at 3010 cm^{-1} and 2986 cm^{-1} correspond to an alkyl chain. The intense peak at 1740 cm^{-1} corresponds to the reaction between acetic acid and TTIP in the formation of the ester in a sol-gel reaction. In the doped TiO$_2$, the vibration band at a position below 600 cm^{-1} is corresponding to the bending mode of the metal oxide [20].
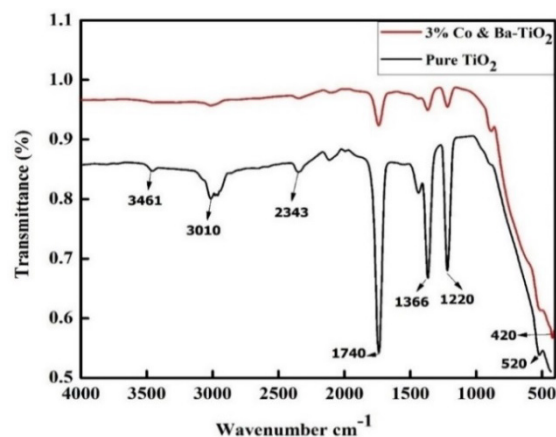
Fig. 5. FTIR spectra of TiO$_2$ and Ba-Co co-doped TiO$_2$ nanoparticles.

SEM studies

The morphologies of synthesized nanoparticles were analyzed through scanning electron microscopy. Figures 6a and 6b show the SEM images of undoped TiO$_2$ and doped TiO$_2$ NPs, respectively. The undoped TiO$_2$ clearly shows rough spherical morphology with small particle agglomeration. In the doped TiO$_2$ NPs slightly larger blocks of agglomerated particles with irregular morphology are present as compared to undoped TiO$_2$.
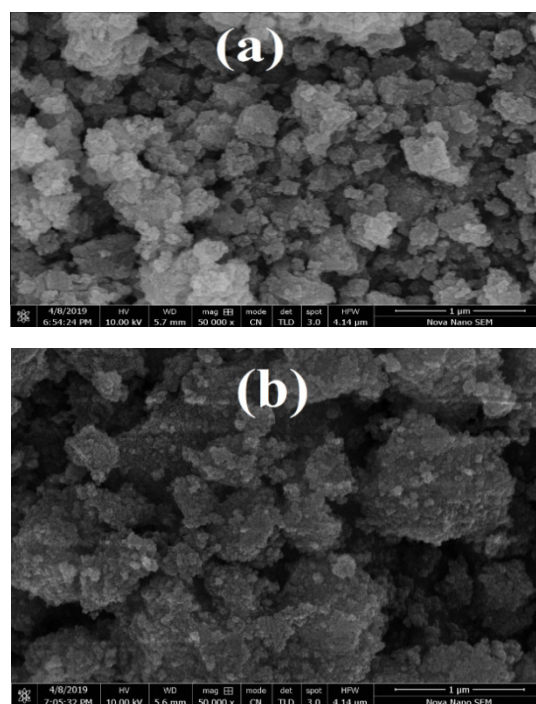
Fig. 6. SEM images of (a) TiO$_2$ and (b) barium and cobalt co- doped TiO$_2$ nanoparticles.

EDX studies

Elemental composition of barium and cobalt co-doped TiO_2 nanoparticles was studied using EDX to investigate the presence of elements in the synthesized nanoparticles as shown in Figure 7. Table 5 summarized the chemical composition of the obtained powders. The results show that the ratio of dopants present in the sample is in accordance with the theoretical value.
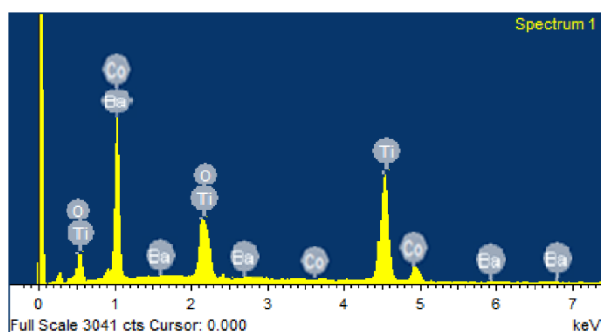
Fig. 7. EDX spectrum of Ba-Co doped TiO_2 nanoparticles.

Table 5. EDX composition of Ba-Co doped TiO_2 nanoparticles.

Sample	wt% (O)	wt% (Ti)	wt% Dopant (Ba & Co)
Ba & Co co-doped TiO_2	59.95	37.08	2.97

Mostly the titanium dioxide is doped with transition metals because the latter possess incomplete d-orbitals with variable oxidation state which enhance the photocatalytic activity of doped nanoparticles. An example is the capability of cobalt and barium to give Co^{2+}, Co^{3+} and Ba^{2+}, Ba^{3+} which retard the recombination of photo-generated carriers.

Due to the comparable atomic radii of cobalt and titanium, cobalt acts as a charge snare in the TiO_2 crystal.TiO_2 doping with such metals changes the optical band gap [21]. The photocatalytic degradation of wastewater containing organic dye under UV light was done using cobalt and barium doped TiO_2. The combination of cobalt and barium with TiO_2 tapers the titanium oxide band gap and

causes a shifting of the absorption edge. The above discussed characteristic of Co and Ba doped TiO_2 improves the photocatalytic degradation of the organic dye.

Photocatalytic degradation of the dye

Effect of irradiation time. The photocatalytic degradation of Coomassive brilliant blue dye was monitored under UV-light at different time intervals ranging from 20 to 280 min. First the experiment was carried out under visible light irradiation but the degradation was not so fruitful. The synthesized undoped TiO_2 and Co-Ba co-doped photocatalyst were used for the degradation of Coomassive brilliant blue dye. About 0.01 mg of undoped TiO_2 and cobalt-barium co-doped TiO_2 were used for the degradation of same dye. Separate solutions of dye were taken in a 150 ml beaker.

The prepared dye solution was kept in a locally designed photoreactor chamber under constant stirring using a magnetic bar with a speed of 60 rpm. About 3 ml was collected from each sample after an interval of 20 min. In the intervals of 20 min all the reaction mixture was collected up to 240 min duration. After that each sample was centrifuged and analyzed using UV spectrophotometry. Initially the degradation of Coomassive brilliant blue was very low both for undoped TiO_2 and Co-Ba co-doped TiO_2 as is evident from the data in Table 6 because a smaller number of hydroxyl radicals was formed due to slow bond cleavage. When irradiation continued, around 48% degradation was observed in 40 min [22]. The absorption spectrum showed that 93% degradation took place in case of Co-Ba co-doped photo catalyst in 240 min, where 70% dye degradation was observed for undoped TiO_2 photocatalyst at the same interval of time.

The results showed that the highest degradation of Coomassive brilliant blue dye was observed using Co-Ba co-doped TiO_2, which is comparatively greater than that of undoped TiO_2. Table 6 and Figures 8 and 9 show the comparative % degradation of Coomassive brilliant blue dye with increasing time using Co-Ba co-doped TiO_2 and undoped TiO_2 photocatalyst.

Table 6. Comparative % degradation of Coomassive brilliant blue dye with increasing time using Co-Ba co-doped TiO_2 and undoped TiO_2 photocatalyst.

Time, (minutes)	20	40	60	80	100	120	140	160	180	200	220	240
% Degradation using Co-Ba co-doped TiO_2	47	48	48	51	56	60	60	66	70	74	88	93
% Degradation using undoped TiO_2	47	48	48	51	56	56	60	60	64	66	67	77
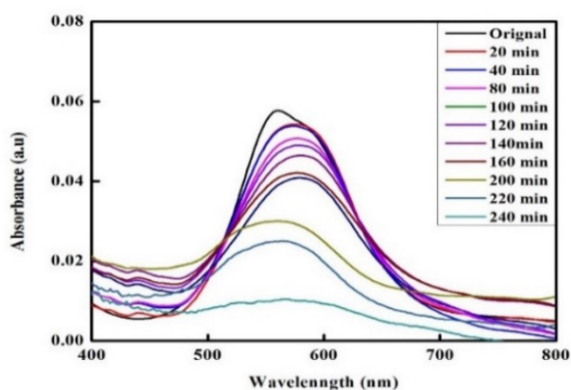
Fig. 8. Comparative % degradation of Coomassive brilliant blue dye with increasing time, using TiO$_2$ photocatalyst.
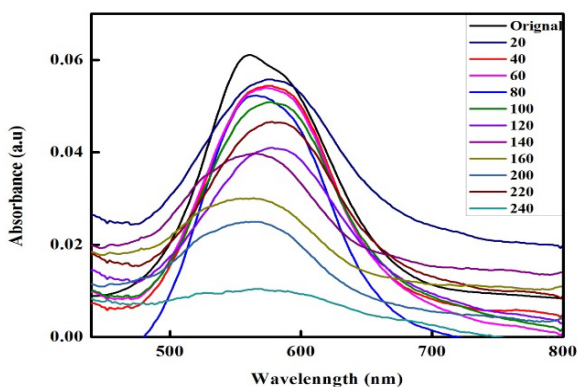
Fig. 9. Comparative % degradation of Coomassive brilliant blue dye with increasing time using Co-Ba co-doped TiO$_2$ photocatalyst.

Effect of dye concentration. The adsorption of dye molecules takes place at the surface of the photocatalyst. During the process of photocatalysis, the dye concentration should no+t be in the bulk of the solution but react with the present amount of photo catalyst in the given solution. In this study different concentrations of Coomassive brilliant blue dye were used in the course of experimentation keeping the amount of photocatalyst and irradiation time constant. Exactly 0.01 mg of both Co-Ba co-doped and undoped TiO$_2$ photocatalyst were used for different initial concentrations of Coomassive dye ranging from 10 ppm to 50 ppm. The data obtained during the experiment and the outcome of the process are presented in Table 7 and Figures 10 and 11.

It was found that with increase in the initial concentration of the Coomassive brilliant blue dye the % degradation decreases. When the concentration of Coomassive brilliant blue dye increased from 10 ppm, a stronger interaction between dye molecule and photocatalyst took place

which formed a large number of intermediate reactants that covered all the surface of the photocatalyst and protected it from further engagement, as a result the formation of hydroxyl radicals decreased. It should be considered that the water changes its physical property and becomes turbid due to higher concentration of dye by blocking the energetic photon to reach and activate the photocatalyst. After that there is no active site present here for the absorption of water to generate the hydroxyl ion which plays an important role in the degradation of dye [23, 24]. The percent degradation of the dye obtained by using different concentrations is shown in Table 7. It can be seen from the table that with an increase in concentration of dye, the active sites of the surface are occupied and ultimately more dye molecules take possession on the surface of the catalyst and screen the catalyst from upcoming light photons, which in turn decreases the approach of photon to reach the dye solution.

Fig. 10. Comparative % degradation of Coomassive
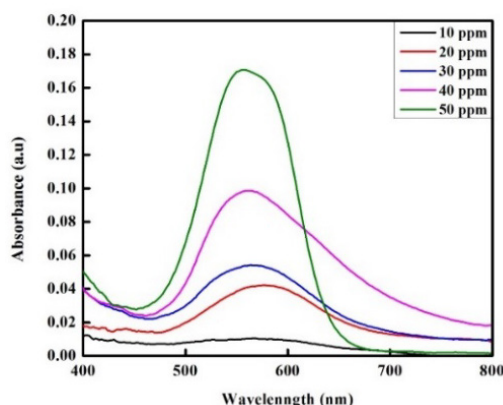
brilliant blue dye with increasing dye concentration using 0.01 mg of TiO$_2$ photocatalyst

The following table shows the comparative % degradation of Coomassive brilliant dye with increasing concentration of the dye from 10 ppm to 50 ppm using Co-Ba co-doped TiO$_2$ and undoped TiO$_2$photocatalyst. Again, it is clear that at low concentration (10 ppm) the dye degradation was maximum (94 %) in case of doped TiO$_2$ and 77% in case of undoped TiO$_2$. The rate of degradation decreased with increasing concentration of the dye as evident from the given tables and figures.

Table 7. Comparative % degradation of Coomassive brilliant blue dye with increasing dye concentration using Co-Ba co-doped TiO$_2$ and undoped TiO$_2$photocatalyst.

Concentration (ppm)	10	20	30	40	50
% Degradation using undoped TiO$_2$	77	75	73	71	59
% Degradation using Co-Ba co-doped TiO$_2$	94	83	77	75	60
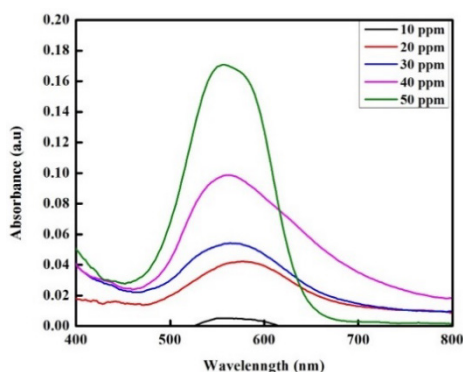
Fig. 11. Comparative % degradation of Coomassive brilliant blue dye with increasing dye concentration using 0.01 mg of Co-Ba co-doped TiO₂photocatalyst.

Effect of catalyst dosage. The catalyst amount plays an important role in photocatalytic degradation of dye. The degradation process of dye must be investigated at different amounts of catalyst because a little increase or decrease on amount of catalyst can affect the rate of dye degradation. This is due to the fact that the increase in the amount of photocatalyst generates a large number of active sites on its surface and increases the number of hydroxyl radicals in the solution mixture. To study the effect of photocatalyst dosage; to the various solutions (10 ppm) of Coomassive brilliant blue dye different weights ranging from 0.01 mg to 0.05 mg of the catalysts were used. The experiment was carried out under UV light and the degradation time was 240 min. Degradation was noted using 0.01 mg, 0.02 mg, 0.03 mg, 0.04 mg, and 0.05 mg of undoped TiO₂ photocatalyst. The maximum degradation (85.5%) was obtained using 0.01 mg of TiO₂ photocatalyst.

After that when increased the amount of undoped TiO₂ catalyst up to 0.02 mg, 0.03 mg, 0.04 mg, 0.05 mg the degradation was found to decrease: 77%, 54%, 48%, and 38%, respectively (Table 8 and Figure 12).

For the same concentration of dye,0.01 mg to 0.06 mg of Co-Ba-doped TiO₂ catalyst was used and 85%, 77%, 77%, 89%, and 95% degradation was observed (Table 8 and Figure 13). Using 0.05 mg of Co-Ba-doped TiO₂ 99.5% degradation was observed while using 0.01 mg of undoped TiO₂ it was 85.5%. In case of undoped TiO₂ it was observed that by increasing catalyst amount the degradation rate decreased. The reason behind is that the solution becomes turbid which covers all the surface of catalyst and forms a suspension which does not allow the photons to reach the surface of TiO₂nphotocatalyst and generate hydroxyl radicals [25, 26].
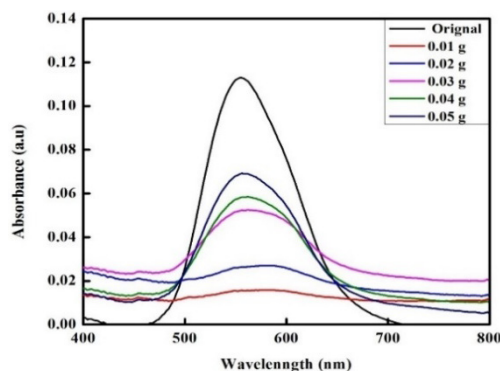
Fig. 12. Comparative % degradation of Coomassive brilliant blue dye with catalyst dose using undoped TiO₂ photocatalyst.

Table 8. Comparative % degradation of Coomassive brilliant blue dye with increasing amount of undoped TiO₂ and Co-Ba co-doped TiO₂.

Catalyst amount (mg)	0.01	0.02	0.03	0.04	0.05	0.06
% Degradation using undoped TiO₂	85.5	77	54	48	38	30
% Degradation using Co-Ba co-doped TiO₂	85	77	77	89	95	88

Table 9. Percent degradation obtained at various pH values by using undoped TiO₂ and Co-Ba co-doped TiO₂photocatalyst.

pH value	3	4	5	8	9
% Degradation using undoped TiO₂	85	82	78	69	51
% Degradation using Co-Ba co-doped TiO₂	92	84	81	76	49

Fig. 13. Comparative % degradation of Coomassive brilliant+ blue dye with catalyst dose using Co-Ba co-doped TiO₂ photocatalyst.

The increase in degradation rate of Co-Ba-doped photocatalyst by increasing the amount from 0.01 mg to 0.05 mg can be explained in terms of generation of a large number of active sites on the surface of the doped photocatalyst and the uncovered surface of the catalyst for UV radiation whereas a great number of photons are available to reach catalyst surface and generate a large number of OH radicals which is responsible for typical discoloration. Furthermore, decrease occurred in the degradation of dye when we increased the catalyst amount from certain optimal level.

From Figure 13 it is clear that with increase in the amount of Co-Ba co-doped photocatalyst an increase in % degradation of CBB occurred.

Effect of pH. pH is the most essential parameter, therefore the degradation of Coomassive dye was investigated at various pH values. From the standard stock solution of Coomassive brilliant blue dye 100 ml of different solutions each having a concentration of 10 ppm were prepared. The pH was adjusted to 3, 4, 5, 6, 8 and 9.

The pH of Coomassive dye solution was calibrated by using 0.1 molar HCl and 0.1 molar NaOH earlier in the experiment. The natural pH value of Coomassive brilliant blue dye is 5.5 which shows its amphoteric character so that it may generate positive or negative charge on its surface during degradation process. The results showed that maximum degradation occurred at pH below 5 which indicates that the optimum pH for degradation was acidic due to the formation of a cation moiety (like hydronium ion) upon protonation which increases its oxidizing ability thus maximum degradation 85% was observed at pH=3 while in a basic medium (pH=9) it was 51% (Figure 15). The effect of proton and hydroxyl is given below:
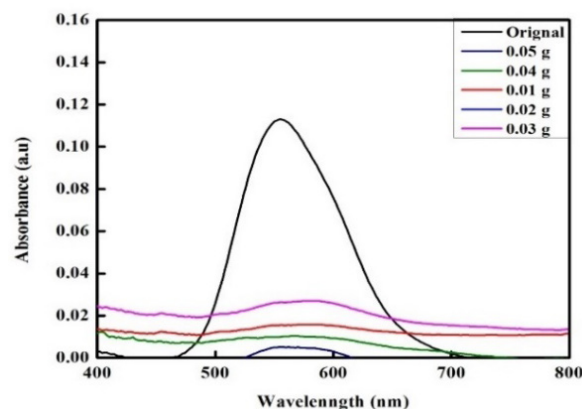
Fig. 14. Comparative % degradation of Coomassive brilliant blue dye with pH using 0.05 g of undoped TiO₂.

$$TiOH + H^+ \longrightarrow TiOH_2^+$$

$$TiOH_2^+ + H_2O \longrightarrow TiOH + OHTiO$$

The reason behind this is that in acidic medium the titania surface gets protonated and becomes positively charged while in alkaline medium the surface is covered by electrons and becomes negatively charged.
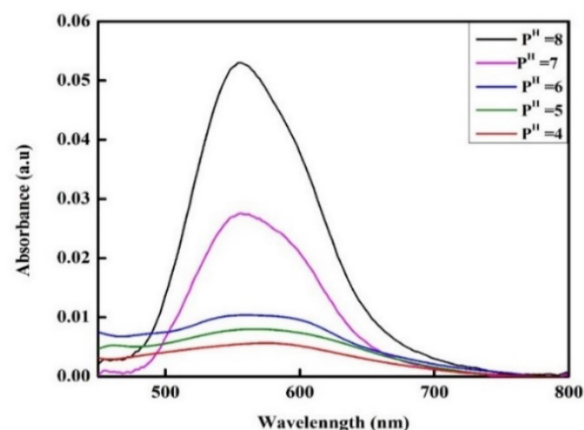
Fig. 15. Comparative % degradation of Coomassive brilliant blue dye with pH using 0.05 g of Co-Ba co-doped TiO₂ photocatalyst.

The higher catalytic activity of TiO₂ photocatalyst is reported in acidic medium and it acts as a Lewis acid. However, a higher concentration of H⁺ can also lower the rate of the reaction from the optimum level. In the presence of a positive charge TiO₂ shows good oxidizing activity. In this case the Coomassive dye acts as a Lewis base and easily adsorbs on the surface of anionic TiO₂ catalyst. This helps the accumulation of the dye at the lower pH. In basic conditions this type of complexation does not take place because of the comparable adsorption of hydroxyl group and the Coomassive dye molecule. In addition, electronic repulsion occurs because of

indirect charge of the catalyst with the dye molecules. In case of Co-Ba co-doped TiO_2 photocatalyst efficient degradation of Coomassive dye occurs in acidic medium (pH=3) - the degradation efficiency of dye is 92% while in basic medium (pH=9) it equals 49% (Figure 15). The reason behind the higher degradation at lower pH could be rationalized by the iso-electric point of TiO_2. It is known from the literature survey that the exact zero-point charge of Co and Ba co-doped $TiO_2$is at pH 6.8. Therefore, at a pH lower than 6.8 the surface of TiO_2 becomes positively charged, and will negatively charge at a pH higher than 6.8. On this justification at pH<6.8 the concentration of positive charges increases on the surface of catalyst. As a result, a higher photocatalytic degradation takes place at acidic pH due to the positively charged surface of the doped photocatalyst and generation of a higher concentration of hydroxyl radicals which are responsible to increase the degradation speed in acidic environment. However, the decrease in decolorization efficiency at basic pH is due to the presence of negative charges at the surface of the doped photocatalyst. The available negative charge causes electrostatic repulsion among the negatively charged Coomassive dye and TiO_2 nanoparticles. It follows from the above discussion that the degradation of Coomassive dye decreases in alkaline medium and increases in acidic medium, the maximum degradation being reported at pH=3 using both undoped and doped titanium dioxide photocatalyst [27, 28]. The % degradation obtained at various pH values is briefly presented in Table 9.

CONCLUSIONS

By doping with Co and Ba the band gap of TiO_2 NPs decreased. Using bare and co-doped TiO_2 NPs for the photocatalytic degradation of Coomassive brilliant blue dye the percent degradation increased with increase in the irradiation time and decreased with increase in the dye concentration. Increasing the amount of co-doped TiO_2 NPs the rate of degradation increased while in case of bare TiO_2 it decreased. Higher degradation was noticed at low pH while it decreased with increase in pH. Co-Ba-doped TiO_2 NPs can effectively be used for the degradation of Coomassive brilliant blue dye in aqueous medium.

Conflict of Interest
There is no conflict of interest between the authors.

REFERENCES

1. Q. Sun, K. Li, S. Wu, B. Han, L. Sui, L. Dong, *New J. Chem.*, **44**, 1942 (2020).
2. M. Rauf, S. Ashraf, S. Alhadrami, *Dyes and Pigments*, **66**, 197 (2005).
3. E. Pino, C. Calderón, F. Herrera, G. Cifuentes, G. Arteaga, *Fron. Chemist.*, **8**, 365 (2020).
4. A. Ajmal, I. Majeed, R.N. Malik, H. Idriss, M.A. Nadeem, *RSC Adv.*, **4**, 37003 (2014).
5. A. Kumar, G. Pandey, *Mater. Sci. Eng. Int. J.*, **1**, 1 (2017).
6. Y. Li, W. Wang, F. Wang, L. Di, S. Yang, S. Zhu, Y. Yao, C. Ma, B. Dai, F. Yu, *Nanomater.*, **9**, 720 (2019).
7. M. Okano, K. Itoh, A. Fujishima, K. Honda, *J. Electrochem. Soc.*, **134**, 837 (1987).
8. M.B. Mukhlish, F. Najnin, M.M. Rahman, M. Uddin, *J. Sci. Res.*, **5**, 301 (2013).
9. M. Amini, M. Ashrafi, *Nanochem. Res.*, **1**, 79(2016).
10. G. Sadanandam, K. Lalitha, V.D. Kumari, M.V. Shankar, M. Subrahmanyam, *Int. J.Hydrogen Energy*, **38**, 9655 (2013).
11. C. Lv, X. Lan, L. Wang, Q. Yu, M. Zhang, H. Sun, J. Shi, *Catal. Sci. Technol.*, **9**, 6124 (2019).
12. P. V. Kamat, Photophysical, photochemical and photocatalytic aspects of metal nanoparticles, ACS Publications, 2002.
13. D. S. Meshesha, R. C. Matangi, S. R. Tirukkovalluri, S. Bojja, *South Afr. J. Chem. Eng.*, **23**, 10 (2017).
14. X. Hong, Z. Wang, W. Cai, F. Lu, J. Zhang, Y. Yang, N. Ma, Y. Liu, *Chem. Mater.*, **17**, 1548 (2005).
15. M. A. Islam, M.J. Haither, I. Khan, M. Islam, *IOSR. Electric Electron Eng.*, **3**, 18 (2012).
16. V. Manikandan, A.K. Palai, S. Mohanty, S.K. Nayak, *J. Photochem. Photobiol. B: Biology*, **183**, 397 (2018).
17. M Ahmed, E.E. El-Katori, Z.H. Gharni, *J. Alloys Comp.*, **553**, 19 (2013).
18. J. Haider, Z.N. Jameel, S.Y. Taha, *Eng. Technol. Jour.*, **33**, 761 (2015).
19. E. Filippo, C. Carlucci, A.L. Capodilupo, P. Perulli, F. Conciauro, G. A. Corrente, G. Gigli, G. Ciccarella, *Mater. Res.*, **18**, 473 (2015).
20. A. Caricato, S. Capone, G. Ciccarella, M. Martino, R. Rella, F. Romano, J. Spadavecchia, A. Taurino, T. Tunno, D. Valerini, *Appl. Surf. Sci.*, **253**, 7937 (2007).
21. S. Salvi, P. Lokhande, H. Mujawar, Photodegradation of Rhodamine 6G dye by Cd, Sr doped ZnO photocatalyst, synthesized by mechanochemical method, International Conference on Communication and Signal Processing 2016 (ICCASP 2016), Atlantis Press, 2016.
22. A. Dodd, A. McKinley, T. Tsuzuki, M. Saunders, *Mater. Chem.Phys.*, **114**, 382 (2009).
23. N. Daneshvar, D. Salari, A. Khataee, *J. Photochem. Photobiol. A: Chemistry*, **162**, 317 (2004).
24. Z. Mengyue, C. Shifu, T. Yaowu, *J. Chem. Technol. Biotechnol.*, **64**, 339 (1995).

25. E. M. Saggioro, A. S. Oliveira, T. Pavesi, C. G. Maia, L. F. V. Ferreira, J.C. Moreira, *Molecules*, **16***, 10370 (2011).
26. K.M. Reza, A. Kurny, F. Gulshan, *Appl. Water Sci.,* **7***, 1569 (2017).
27. B. Viswanathan, *Curr. Catal.,***7**, 99 (2018).
28. A. M. Santhosh, K, K. M.Yogendra, I.H. Mahadevan, N. Mallikarjuna, Madhusudhana, *J. Technol. Innov. Res.(JETIR)*, **5**, 2349 (2018).